ISSN 1674-1056
http://cpb.iphy.ac.cn
http://iopscience.iop.org/cpb
中国物理 B
Chinese Physics
中国物理
Chinese Physics B

Room-temperature large photoinduced magnetoresistance in semi-insulating gallium arsenide-based device

Xiong He(何雄), Zhi-Gang Sun(孙志刚)
Citation: Chin. Phys. B . 2018, 27(6): 067204. **doi:** 10.1088/1674-1056/27/6/067204

Journal homepage: http://cpb.iphy.ac.cn; http://iopscience.iop.org/cpb

What follows is a list of articles you may be interested in

Recent observations of negative longitudinal magnetoresistance in semimetal

Xi-Tong Xu(许锡童), Shuang Jia(贾爽)
Chin. Phys. B . 2016, 25(11): 117204. **doi:** 10.1088/1674-1056/25/11/117204

Large linear magnetoresistance in a new Dirac material $BaMnBi_2$

Yi-Yan Wang(王义炎), Qiao-He Yu(郁巧鹤), Tian-Long Xia(夏天龙)
Chin. Phys. B . 2016, 25(10): 107503. **doi:** 10.1088/1674-1056/25/10/107503

Manipulating magnetic anisotropies of Co/MgO(001) ultrathin films via oblique deposition

Syed Sheraz Ahmad, Wei He(何为), Jin Tang(汤进), Yong Sheng Zhang(张永圣), Bo Hu(胡泊), Jun Ye(叶军), Qeemat Gul, Xiang-Qun Zhang(张向群), Zhao-Hua Cheng(成昭华)
Chin. Phys. B . 2016, 25(9): 097501. **doi:** 10.1088/1674-1056/25/9/097501

Tunneling magnetoresistance based on a Cr/graphene/Cr magnetotunnel junction

Luan Gui-Ping, Zhang Pei-Ran, Jiao Na, Sun Li-Zhong
Chin. Phys. B . 2015, 24(11): 117201. **doi:** 10.1088/1674-1056/24/11/117201

Field-induced insulator-metal-insulator transitions in low-energy H_2^+ ion-irradiated epitaxial $La_{2/3}Ca_{1/3}MnO_3$ thin films

Wu Zhan-Wen, Li Jie, Li Song-Lin, Zheng Dong-Ning
Chin. Phys. B . 2013, 22(8): 087503. **doi:** 10.1088/1674-1056/22/8/087503

Room-temperature large photoinduced magnetoresistance in semi-insulating gallium arsenide-based device*

Xiong He(何雄) and Zhi-Gang Sun(孙志刚)†

State Key Laboratory of Advanced Technology for Materials Synthesis and Processing, Wuhan University of Technology, Wuhan 430070, *China*

(Received 10 November 2017; revised manuscript received 2 February 2018; published online 10 May 2018)

It is still a great challenge for semiconductor based-devices to obtain a large magnetoresistance (MR) effect under a low magnetic field at room temperature. In this paper, the photoinduced MR effects under different intensities of illumination at room temperature are investigated in a semi-insulating gallium arsenide (SI-GaAs)-based Ag/SI–GaAs/Ag device. The device is subjected to the irradiation of light which is supplied by light-emitting diode (LED) lamp beads with a wavelength in a range of about 395 nm–405 nm and the working power of each LED lamp bead is about 33 mW. The photoinduced MR shows no saturation under magnetic fields (B) up to 1 T and the MR sensitivity S ($S = \mathrm{MR}/B$) at low magnetic field ($B = 0.001$ T) can reach 15 T^{-1}. It is found that the recombination of photoinduced electron and hole results in a positive photoinduced MR effect. This work implies that a high photoinduced S under a low magnetic field may be obtained in a non-magnetic semiconductor device with a very low intrinsic carrier concentration.

Keywords: GaAs, magnetoresistance, carrier recombination

PACS: 72.80.Ey, 75.47.–m, 72.20.Jv **DOI:** 10.1088/1674-1056/27/6/067204

1. Introduction

The magnetoresistance (MR) effect attracts lots of attention because of its great research significance and potential applications in magnetic sensors,[1,2] hard drives,[3] magnetic memory,[4] etc. Comparing with the magnetic materials, the MR effects on the non-magnetic materials, such as Si,[5–16] Ge,[17–20] $NbSb_2$,[21] WTe_2,[22] InAs,[23] CdTe,[24] $Hg_{0.77}Cd_{0.23}Te$,[25] GaAs,[26–30] etc., each present a comparable large MR ratio. Among them, MR devices based on GaAs, which is one of the direct band gap non-magnetic semiconductors, have also attracted a great deal of attention. Previous researches were mainly concentrated on the MR effects at low temperature.[28–30] Subsequently, some room temperature MR effects have been investigated.[26,27] For example, Sun *et al.*[27] found a large room-temperature MR effect in the Au/semi-insulating (SI) GaAs/Au device, reaching 10^5% at 0.8 T. Wang *et al.*[26] observed a diode enhanced MR effect of about 2600% under a magnetic field of 1.2 T in GaAs at room temperature.

Some researches have shown that the semiconductor materials-based MR effects could be significantly enhanced by light irradiation.[31–38] For example, Akinaga *et al.*[32] observed a large photoinduced MR effect of 20% at $B = 0.1$ T in GaAs including nanoscale MnSb islands. Recently, Viana *et al.*[39] obtained photoinduced MR in a p-type SI-GaAs sample. However, the absolute value of photoinduced MR at room temperature was far smaller than 0.5% and the corresponding MR sensitivity ($S = \mathrm{MR}/B$[8]) was far lower than 0.05 T^{-1}. A large ratio of MR at room temperature under a low magnetic field still needs to be further investigated.

In order to obtain a large photoinduced MR and high S under a low magnetic field, we fabricate an SI-GaAs-based Ag/SI–GaAs/Ag device and investigate the photoinduced MR at room temperature. A high photoinduced S (about 15 T^{-1} at $B = 0.001$ T) is obtained and its mechanism is also analyzed.

2. Experiments

In this paper, we used the n-type semi-insulating (SI)-GaAs (provided by Hefei Kejing Materials Technology Co., Ltd.) with a resistivity of 1.42 Ω·cm–1.53×10^8Ω·cm, mobility of 5380 $\mathrm{cm}^2/(\mathrm{V\cdot s})\sim$ 5700 $\mathrm{cm}^2/(\mathrm{V\cdot s})$, and dislocation density of less than 5200 cm^{-2}. The SI–GaAs wafer was single-side polished with a thickness of 0.35 mm. The wafer was cut into a rectangular shape with a length of 7.22 mm and a width of 2.87 mm, and was cleaned by a mixture solution of ammonia, hydrogen peroxide, and deionized water of 1:2:5 volume ratio under ultrasonic vibration. Four silver paste electrodes were aligned along the centerline of the wafer on the polished face (as shown in Fig. 1(a). Figure 1(b) presents the scanning electron micrscopy (SEM) cross-section image of the electrode). As shown in Fig. 1(c), the work function of SI–GaAs (about 4.8 eV) is larger than that of the Ag electrode (about 4.3 eV), so the contact between Ag electrode and SI–GaAs can be regarded as an ohmic contact.

The electronic transport properties of the devices were measured by using a Keithley 6220 current source, Keithely 6485 picoammeter, and Keithley 2182 A voltmeter. In the high resistance measurement mode, the current source provided a

*Project supported by the National Natural Science Foundation of China (Grant Nos. 11574243 and 11174231).

†Corresponding author. E-mail: sun_zg@whut.edu.cn

© 2018 Chinese Physical Society and IOP Publishing Ltd

current range from ±0.1 pA to ±0.1 A, the picoammeter measures the current in a range from ±10 fA to ±21 mA in which the minimum resolution is 10 fA and the voltmeter collects the voltage in a range from ±0.1 nV to ±100 V in which the minimum resolution is 0.1 nV. The electronic transport measurement is illustrated in Fig. 1(a), the excitation illumination supplied by LED lamp beads with the wavelength in a range of about 395 nm–405 nm and the working power of each LED lamp bead was about 33 mW. The distance between the LED lamp beads and the device was about 100 mm and the light was perpendicular to the sample surface and illuminated the whole surface. Only after the stabilization of illumination, were the electrical transport measurements performed under different magnetic fields. The intensity of illumination is linearly dependent on the number of LED lamp beads. Therefore, for simplicity, we denote the illumination intensity as N-LEDs, where N represents the number of the LED lamp beads. The magnetic field (B) was perpendicular to the current and parallel to the sample plane (see Fig. 1(a)). As shown in Fig. 1(d), there were almost no differences among the V–I characteristics of an LED lamp bead under different magnetic fields, indicating that the applied magnetic field has no effect on the intensity of illumination.

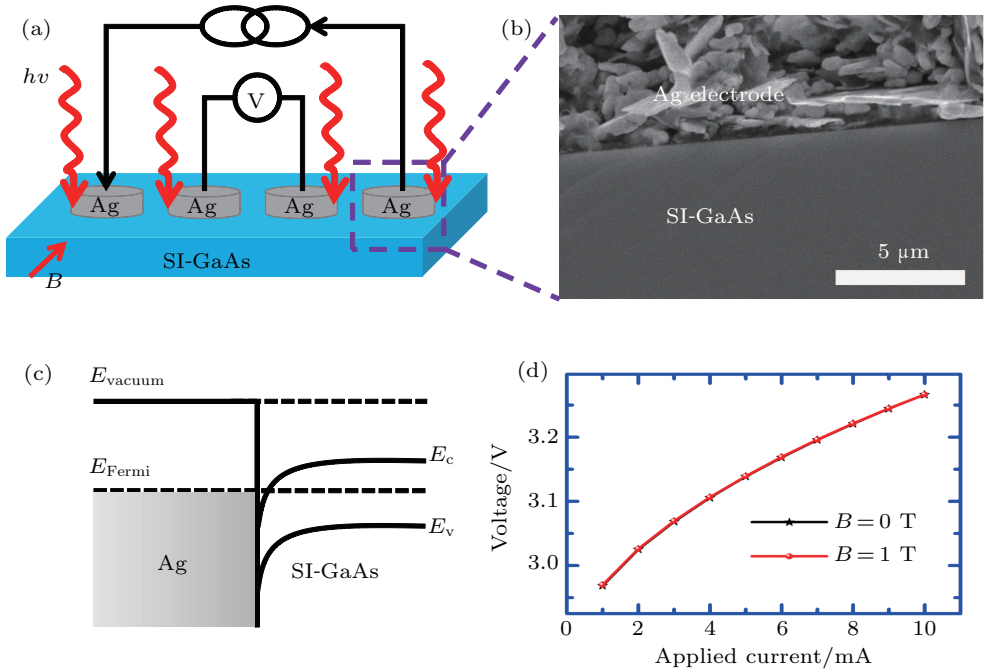


Fig. 1. (color online) (a) Measurement schematic diagram of the SI–GaAs-based device, (b) SEM cross-section image of the electrode, (c) energy diagram of Ag electrode and SI–GaAs semiconductor, and (d) V–I curves of an LED lamp bead under different magnetic fields.

The carrier concentrations were measured by the Van der Pauw method on a 9 mm×9 mm square wafer under the irradiation of different-intensity light. The measurement results showed that the carrier concentrations in the dark, 2-LEDs, and 4-LEDs intensity of illumination environment were about 5.5×10^{9} cm^{-3}, 3.7×10^{11} cm^{-3}, and 5.0×10^{11} cm^{-3}, respectively. The Hall coefficients in the dark, 2-LEDs, and 4-LEDs intensity of illumination were -1.1×10^{9} cm^{3}·C^{-1}, -1.7×10^{7} cm^{3}·C^{-1}, and -1.3×10^{7} cm^{3}·C^{-1}, respectively. The Hall coefficients are negative, indicating that the conductive type of the device is indeed n-type. All the above measurements were obtained at room temperature.

In order to eliminate the influence of Hall effects, we took $V_{\rm even}(B)=[V(B)+V(-B)]/2$ as the real voltage values under magnetic field and calculated the MR ratio from MR $=[V_{\rm even}(B)-V(0)]\times100\%/V(0)$, where $V(B)$, $V(-B)$, and $V(0)$ represented the testing voltage under positive, negative magnetic field, and zero magnetic field, respectively.

3. Results and discussion

Figures 2(a) and 2(b) display the voltage–current (V–I) curves under different-intensity illumination and different magnetic fields (the number of V–I curves under 0.005 T, 0.01 T, 0.05 T, 0.1 T, and 0.5 T are not presented for clarity). As stated in the experimental part, the carrier concentration in the dark is very low, the V–I curves of the device in the dark are hard to obtain. It can be seen from Figs. 2(a) and 2(b) that the V–I curves show linear characteristics under no applied magnetic field. At the same applied current and magnetic field, the voltage under 2-LEDs irradiation is larger than that under 4-LEDs irradiation. As stated above, the carrier concentration under 2-LEDs irradiation is smaller than under 4-LEDs irradiation. Therefore, the larger voltage under 2-LEDs irradiation is mainly attributed to the smaller carrier concentration according to the formula $V=Il/(nq\mu S_0)$, where n, q, and μ are the carrier concentration, the charge of electron, and the carrier mobility, respectively, l and S_0 refer to the length be-

tween the two electrodes in the middle and the cross-sectional area of the sample, respectively.

The V–I curves remain linear an under applied magnetic field and the slope increases with the magnetic field increasing. As shown in Figs. 2(c) and 2(d), the initial voltage, which is the intersection between V–I curves and the y axis, is about zero with or without magnetic field, indicating that the contact between Ag and SI–GaAs is indeed an ohmic contact, which is consistent with the energy band result. Therefore, the MR effect discussed below belongs to the bulk effect. This proves once again that our work focuses on the intrinsic photoinduced MR effect, which is obviously different from the magneto-photogalvanic effect in p–n junctions.[37]

The calculated MR-B curves and corresponding calculated S–B curves are shown in Figs. 2(e) and 2(f). Under 2-LEDs irradiation, with the increase of magnetic fields, the MR increases sharply from about 1.3% under $B = 0.001$ T to 7.6% under 0.1 T and then increases slowly. When the intensity of the illumination is from 4 LEDs, the value of MR increases with applied magnetic field increasing and does not show saturation. It is interesting to observe that the value of MR under 0.001 T can reach about 1.5% (see Fig. 2(f)). Meanwhile, the MR under 4-LEDs irradiation is larger than that under 2-LEDs irradiation. This indicates that a larger photoinduced positive MR can be obtained under a higher intensity of illumination.

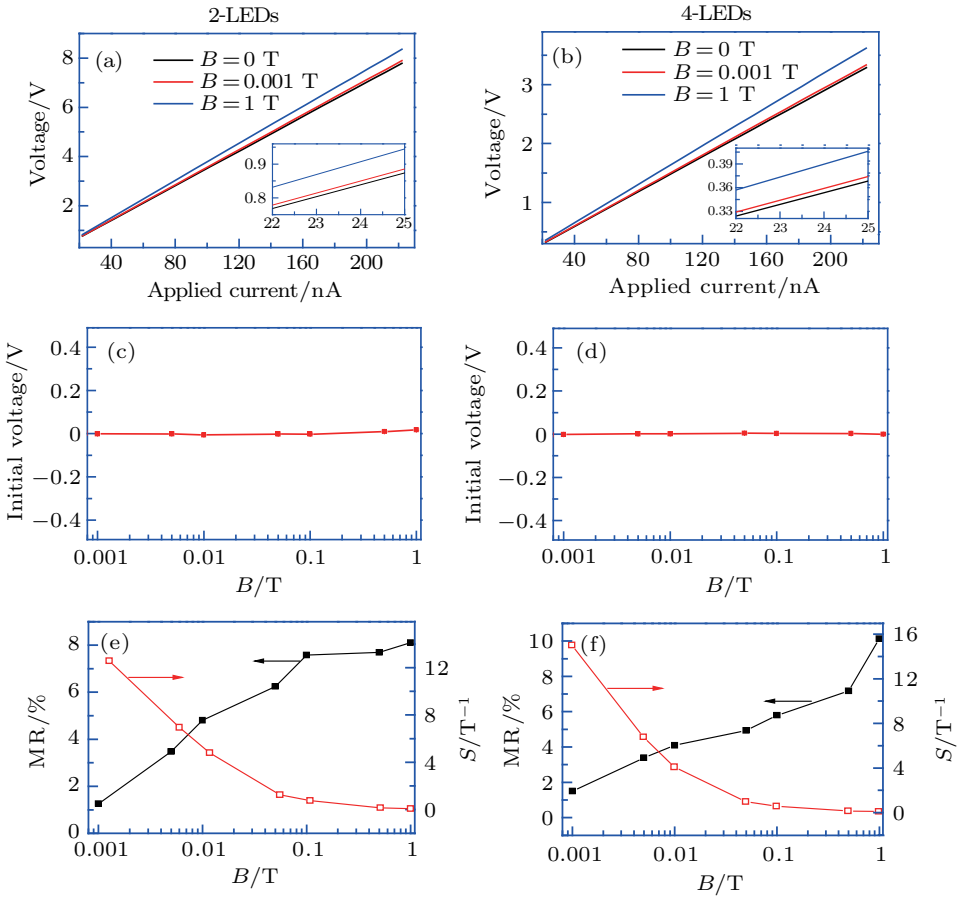


Fig. 2. (color online) [(a) and (b)] V–I characteristics under different magnetic fields, with insets showing magnified parts of curves. [(c) and (d)] Curves of initial voltage versus magnetic field. [(e) and (f)] Calculated MR–B curves and S–B curves at $I = 22$ nA. Curves are obtained under [(a), (c), and (e)] 2-LEDs illumination and [(b), (d), and (f)] 4-LEDs illumination.

As shown in Figs. 2(e) and 2(f), S decreases sharply with applied magnetic field increasing. When $B = 1$ T, the values of S are about 0.08 T^{-1} under 2-LEDs irradiation (see Fig. 2(e)) and about 0.1 T^{-1} under 4-LEDs irradiation (see Fig. 2(f)), respectively. The highest S values are about 13 T^{-1} under 2-LEDs irradiation (see Fig. 2(e)) and about 15 T^{-1} under 4-LEDs irradiation (see Fig. 2(f)), respectively. Under the same applied magnetic field, the value of S under 2-LEDs irradiation is smaller than that under 4-LEDs irradiation, indicating that a higher S value may be observed under higher-intensity illumination. It is worth noting that the obtained S value is at least 3 orders of magnitude higher than that in previous values from GaAs-based devices,[39] higher than those from non-magnetic Si-based devices ($S = 3.15$ T^{-1} at $B = 0.25$ T[8]) and from non-magnetic Ge-based devices ($S \approx 8$ T^{-1} at $B = 0.4$ T[17]), and also higher than the value of S reported by Akinaga *et al.*[32] ($S = 2.5$ T^{-1}, MR = 20%@$B = 0.1$ T) from magnetic doping semiconductor devices. Even though the high value of S ($S > 12$ T^{-1}, MR > 600% at $B < 0.5$ T in GaAs:MnAs granular thin film[40]) was obtained in a magnetic doping semiconductor device, the applied magnetic field was still high. Recently, a large value of S ($S \approx 21.7$ T^{-1}, MR $\approx$ 2600%@$B =$

1.2 T) was found in a GaAs-based device.[26] However, this work was based on the diode enhanced MR effect, which was not an intrinsic effect of GaAs.

There are many physical models of large positive MR effects in non-magnetic semiconductors-based devices, such as the space-charge effects,[7,8,11–14,19] diode-assisted geometry enhanced model,[26,41] band theory,[22] avalanche breakdown model,[6,9,23,27,42] the nano-inhomogeneous model,[15,24] the antilocalization effect,[39] and the carrier recombination effects.[17,43] Among them, the space charge of the space charge effects is from the electron injection[7,8,19] or the intrinsic space-charge region of the p–n junction.[11–14] In the diode-assisted geometry enhanced model, the p–n junction nonlinear electrical transport properties are combined with the geometric effects of the Lorentz force. The band theory explanation usually works under low temperature. Meanwhile, an avalanche breakdown model is generally used in the case of the high energy electron impact ionization. Nevertheless, the MR effect in our work belongs to the bulk effect at room temperature and the carriers are mainly photoinduced electrons and holes. Therefore, the above four models may not be suitable for explaining our present MR effects. Furthermore, under light irradiation conditions, most photoinduced carriers are generated around the surface of SI–GaAs and diffuse into the deep of semiconductors exponentially, resulting in the inhomogeneous distribution of photoinduced carriers in the direction perpendicular to the surface of the sample since the carrier diffusion lengths in GaAs[44] are much smaller than the thickness of our device. Further investigation of the influence of the inhomogeneous distribution of the photoinduced carriers in the direction perpendicular to the surface of the sample is surely required. However, previous researches[15,24] showed that the nano-inhomogeneous model was related to the spatial fluctuation in the donor density. Meanwhile, in our work, the distribution of photoinduced carriers is homogeneous along the surface of the sample. Therefore, the nano-inhomogeneous model may not be suitable to explaining the MR effect in this work. Besides, the antilocalization effect is expected to be stronger in p-type materials,[39] so that is not the case in our device. Interested readers may refer to our recent review article that focuses on the physical models of MR effects in non-magnetic semiconductors.[45] Through the above analysis, we believe that the carrier recombination effect is more applicable to the photoinduced MR effect in this work since the photoinduced electrons and holes are inclined to recombine and can be influenced by the magnetic field.

On the basis of the carrier recombination model, the schematics of the electron/hole recombination under different intensities of light irradiation conditions are shown in Figs. 3(a) and 3(b). When the SI–GaAs-based device is in the dark, the recombination rate of intrinsic electron and hole is very small since their concentrations are very low (see Fig. 3(a)). As shown in Fig. 3(b), under the light irradiation condition, the photoinduced carrier concentration increases sharply. When the magnetic field is applied, the electron and hole are affected by the Lorentz force, increasing the recombination rate, resulting in the decrease of the carrier concentration and increase of the resistivity. Eventually, the positive photoinduced MR is obtained. Compared with the photoinduced carrier concentration under 2-LEDs irradiation, the concentration of photoinduced carrier under 4-LEDs irradiation is high. Therefore, under the same magnetic field, the recombination rate under 4-LEDs irradiation is larger than that under 2-LEDs irradiation, resulting in a larger positive photoinduced MR.

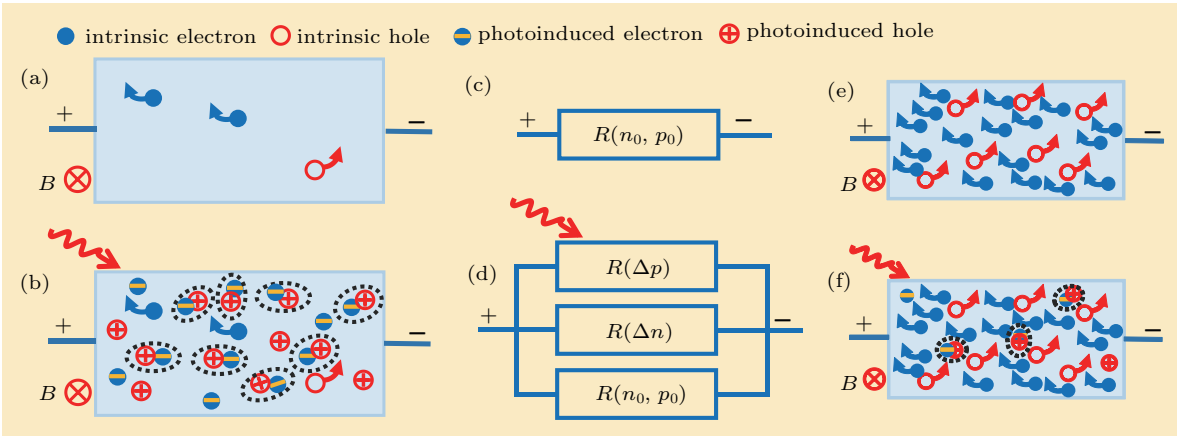


Fig. 3. (color online) Schematics of the photoinduced electron/hole recombination (a) in the dark and under light irradiation condition (b). Equivalent resistance of the device (c) in the dark and (d) under light irradiation. Schematics of a sample with high intrinsic carrier concentration (e) in the dark and (f) the corresponding photoinduced electron/hole recombination under light irradiation condition.

Another interesting phenomenon is that the high value of S is obtained under an extremely low magnetic field (i.e., 0.001 T). As shown in Fig. 3(c), when the device is in the dark conditions, the resistance is denoted as $R(n_0, p_0)$, where n_0 and p_0 are the intrinsic electron and hole concentration, respectively. In the condition of illumination as shown in Fig. 3(d), the equivalent resistance can be regarded as the parallel resistance which consists of $R(n_0, p_0)$, the equivalent re-

sistance $R(\Delta n)$ and $R(\Delta p)$ of photoinduced carrier, where Δn and Δp represent the concentrations of photoinduced electron and hole, respectively. The parallel resistance under illumination is expressed as $R(n_0(B), p_0(B), \Delta n(B), \Delta p(B), B)$, where $n_0(B)$ and $p_0(B)$ are the intrinsic concentrations of electron and hole under magnetic field, respectively, and $\Delta n(B)$ and $\Delta p(B)$ represent photoinduced electron and hole under magnetic field, respectively. Under the irradiation condition, the photoinduced MR can be expressed as

$$\mathrm{MR} = \frac{R(n_0(B), p_0(B), \Delta n(B), \Delta p(B), B)}{R(n_0(0), p_0(0), \Delta n(0), \Delta p(0), 0)} - 1. \tag{1}$$

Besides,

$$= \frac{l}{S_0 q} \frac{1}{\mu_\mathrm{n}(n_0(B)+\Delta n(B)) + \mu_\mathrm{p}(p_0(B)+\Delta p(B))}$$

and $|B| \neq 0$, where μ_n and μ_p represent the mobility of electron and hole, respectively. At room temperature, the mobility of the carrier can be regarded as a constant. Then equation (1) can be transformed into

$$\mathrm{MR} = \frac{\mu_\mathrm{n}(n_0(0)+\Delta n(0)) + \mu_\mathrm{p}(p_0(0)+\Delta p(0))}{\mu_\mathrm{n}(n_0(B)+\Delta n(B)) + \mu_\mathrm{p}(p_0(B)+\Delta p(B))} - 1. \tag{2}$$

If the intrinsic carrier concentration of the sample is very small as shown in Figs. 3(a) and 3(b), in other words, the photoinduced carrier concentration $\Delta n(0)$ and $\Delta p(0)$ are very high, the concentration of photoinduced carrier will be drastically reduced under a low applied magnetic field because of the larger recombination rate of the photoinduced carrier. Therefore, a positive photoinduced MR with a high value of S may be obtained.

On the other hand, if the intrinsic carrier concentration of the sample is very high (see Fig. 3(e)), i.e., n_0 and p_0 are much larger than the values of Δn and Δp, equation (2) will be transformed into

$$\mathrm{MR} = \frac{\mu_\mathrm{n} n_0(0) + \mu_\mathrm{p} p_0(0)}{\mu_\mathrm{n} n_0(B) + \mu_\mathrm{p} p_0(B)} - 1. \tag{3}$$

It can be seen from Eq. (3) that the MR mainly depends on the variation of carrier concentration at the equilibrium, and is hardly influenced by photoinduced carrier concentration. Therefore, the recombination rate for the high intrinsic carrier concentration condition will be smaller than that for the low intrinsic carrier concentration condition under the same strength of applied magnetic field (see Figs. 3(b) and 3(f)). Eventually, the values of photoinduced MR and S will be smaller. Thus, it indicates that the high value of photoinduced S may be obtained in a non-magnetic semiconductor-based device with low intrinsic carrier concentration.

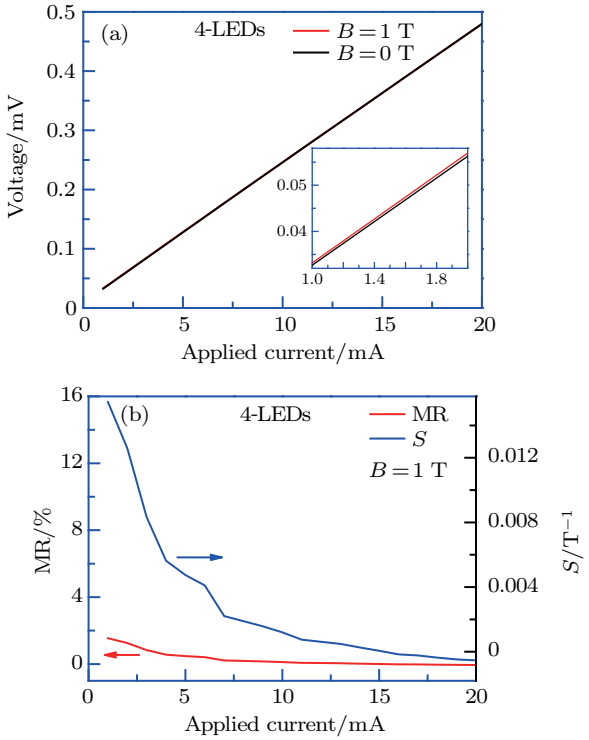


Fig. 4. (color online) (a) V–I characteristic curve of the In/n-GaAs/In device under different magnetic fields and 4-LEDs intensity of illumination, with inset showing magnified part of the curves. (b) Calculated MR–I and S–I curves under 1 T.

In order to further analyze the effect of intrinsic carrier concentration on the photoinduced MR, we fabricate an In/n-GaAs/In device with a higher intrinsic carrier concentration of about 3×10^{17} cm^{-3}–4×10^{17} cm^{-3} and the geometric dimensions remain the same. We use the same measurement method to measure the electronic transport properties of the device under 4-LEDs irradiation. The results are shown in Fig. 4(a). In Fig. 4(a), one can easily find that the V–I curves show linear characteristics and the initial voltage is about zero with or without magnetic field, indicating that the contact between In electrode and n-GaAs is an Ohmic contact. Similarly, the photoinduced MR effects in the In/n-GaAs/In device can also be considered as a bulk effect. The other one is that the resistance of the n-GaAs-based device is obviously smaller than that of the SI–GaAs-based device (see Fig. 2(b)), which is mainly attributed to the different concentrations of the two GaAs-based devices. Figure 4(b) shows the calculated MR–I and corresponding calculated S–I curves under 1 T. It is seen that the MR and the corresponding S show their decreasing with current increasing, and the maximum values of photoinduced MR and the corresponding S are about 1.5% and 0.015 T^{-1}, respectively. Compared with the values of MR and S of the SI–GaAs-based device under the same conditions (see Fig. 2(f)), the values of MR and S of the n-GaAs-based device are about one order of magnitude smaller, respectively. Meanwhile, according to a previous result,[10] the highest non-photoinduced MR is obtained in the silicon device with a low acceptor concentration. Consequently, based on the above investigations, it is more reasonable to believe that in a

non-magnetic semiconductor-based device, low intrinsic carrier concentration may be beneficial to obtaining larger photoinduced MR and S.

4. Conclusions

In this work, a photoinduced positive MR with large MR sensitivity have been observed in the SI–GaAs-based Ag/SI–GaAs/Ag device with low intrinsic carrier concentration at room temperature. The MR value increases with applied magnetic field increasing. When the intensity of the illumination increases, the value of S increases, and the highest S value reaches 15 T^{-1} under 0.001 T. Mechanism analysis shows that the positive photoinduced MR is mainly due to the recombination of photoinduced electron and hole. This paper indicates that a high photoinduced S under a low magnetic field may be obtained in a non-magnetic semiconductor device with low intrinsic carrier concentration.

References

[1] Reig C, Cubells-Beltran M D and Munoz D R 2009 *Sensors* **9** 7919
[2] Lenz J E 1990 *Proc. IEEE* **78** 973
[3] Daughton J M 1999 *J. Magn. Magn. Mater.* **192** 334
[4] Martins L, Ventura J, Ferreira R and Freitas P P 2017 *Appl. Surf. Sci.* **424** 58
[5] Luo Z C, Zhang X Z, Xiong C Y and Chen J J 2015 *Adv. Funct. Mater.* **25** 158
[6] Schoonus J J H M, Bloom F L, Wagemans W, Swagten H J M and Koopmans B 2008 *Phys. Rev. Lett.* **100** 127202
[7] Delmo M P, Yamamoto S, Kasai S, Ono T and Kobayashi K 2009 *Nature* **457** 1112
[8] Delmo M P, Shikoh E, Shinjo T and Shiraishi M 2013 *Phys. Rev. B* **87** 245301
[9] He X, Sun Z G, Pang Y Y and Li Y C 2017 *J. Appl. Phys.* **121** 114501
[10] Schoonus J J H M, Haazen P P J, Swagten H J M and Koopmans B 2009 *J. Phys. D: Appl. Phys.* **42** 185011
[11] Wang T, Yang D Z, Si M S, Wang F C, Zhou S M and Xue D S 2016 *Adv. Electron. Mater.* **2** 1600174
[12] Yang D Z, Wang T, Sui W B, Si M S, Guo D W, Shi Z, Wang F C and Xue D S 2015 *Sci. Rep.* **5** 11096
[13] Wang T, Si M S, Yang D Z, Shi Z, Wang F C, Yang Z L, Zhou S M and Xue D S 2014 *Nanoscale* **6** 3978
[14] Yang D Z, Wang F C, Ren Y, Zuo Y L, Peng Y, Zhou S M and Xue D S 2013 *Adv. Funct. Mater.* **23** 2918
[15] Porter N A and Marrows C H 2012 *Sci. Rep.* **2** 565
[16] Wan C H, Zhang X Z, Gao X L, Wang J M and Tan X Y 2011 *Nature* **477** 304
[17] Chen J J, Piao H G, Luo Z C and Zhang X Z 2015 *Appl. Phys. Lett.* **106** 173503
[18] Chen J J, Piao H G, Luo Z C, Xiong C Y and Zhang X Z 2016 *Chin. Phys. Lett.* **33** 047501
[19] Chen J J, Zhang X Z, Luo Z C, Wang J M and Piao H G 2014 *J. Appl. Phys.* **116** 114511
[20] Zhang K, Li H H, Grünberg P, Li Q, Ye S T, Tian Y F, Yan S S, Lin Z J, Kang S S, Chen Y X, Liu G L and Mei L M 2015 *Sci. Rep.* **5** 14249
[21] Wang K F, Graf D, Li L J, Wang L M and Petrovic C 2015 *Sci. Rep.* **4** 7328
[22] Ali M N, Xiong J, Flynn S, Tao J, Gibson Q D, Schoop L M, Liang T, Haldolaarachchige N, Hirschberger M, Ong N P and Cava R J 2014 *Nature* **514** 205
[23] Velichko A V, Makarovsky O, Mori N, Eaves L, Krier A, Zhuang Q and Patanè A 2014 *Phys. Rev. B* **90** 085309
[24] Ahmad F R 2015 *Appl. Phys. Lett.* **106** 012109
[25] Liu X Z, Yu G, Wei L M, Lin T, Xu Y G, Yang J R, Wei Y F, Guo S L, Chu J H, Rowell N L and Lockwood D J 2013 *J. Appl. Phys.* **113** 013704
[26] Wang J M, Zhang X Z, Wan C H, Piao H G, Luo Z C and Xu S Y 2013 *J. Appl. Phys.* **114** 034501
[27] Sun Z G, Mizuguchi M, Manago T and Akinaga H 2004 *Appl. Phys. Lett.* **85** 5643
[28] Papadakis S J, Poortere E P D, Shayegan M and Winkler R 2000 *Phys. Rev. Lett.* **84** 5592
[29] Tremblay F, Pepper M, Ritchie D, Peacock D C, Frost J E F and Jones G A C 1989 *Phys. Rev. B* **39** 8059
[30] Halbo L and Sladek R J 1968 *Phys. Rev.* **173** 794
[31] Shon Y, Yuldashev S U, Fan X, Fu D, Kwon Y H, Hong C Y and Kang T W 2001 *Jpn. J. Appl. Phys.* **40** 3082
[32] Akinaga H, Mizuguchi M, Ono K and Oshima M 2000 *Appl. Phys. Lett.* **76** 2600
[33] Yue Z J, Zhao K, Ni H, Zhao S Q, Kong Y C, Wong H K and Wang A J 2011 *J. Phys. D: Appl. Phys.* **44** 095103
[34] Xi J F, Ni H, Zhao K, Lu H B, Guo E, He M, Jin K J, Zhou Y L, Yang G Z, Xiao L Z and Zhang Z W 2016 *Appl. Phys. A* **122** 489
[35] Volkov N V, Tarasov A S, Eremin E V, Baron F A, Varnakov S N and Ovchinnikov S G 2013 *J. Appl. Phys.* **114** 093903
[36] Wang S H, Wang W X, Zou L K, Zhang X, Cai J W, Sun Z G, Shen B G and Sun J R 2014 *Adv. Mater.* **26** 8059
[37] Zhou J K, Wang T, Wang W, Chen S W, Cao Y, Liu H P, Si M S, Gao C X, Yang D Z and Xue D S 2016 *Appl. Phys. Lett.* **109** 232404
[38] Sun Z G, Pang Y Y, Hu J H, He X and Li Y C 2016 *Acta Phys. Sin.* **65** 097301 (in Chinese)
[39] Viana E R, Ribeiro G M, Oliveira A G d, Peres M L, Rubinger R M and Rubinger C P L 2012 *Mater. Res.* **15** 530
[40] Yokoyama M, Ogawa T, Nazmul A M and Tanaka M 2006 *J. Appl. Phys.* **99** 08D502
[41] Luo Z C and Zhang X Z 2015 *J. Appl. Phys.* **117** 17A302
[42] Lee J, Joo S, Kim T, Kim K H, Rhie K, Hong J and Shin K H 2010 *Appl. Phys. Lett.* **97** 253505
[43] Joo S, Kim T, Shin S H, Lim J Y, Hong J, Song J D, Chang J, Lee H W, Rhie K, Han S H, Shin K H and Johnson M 2013 *Nature* **494** 72
[44] Casey H C, Miller B I and Pinkas E 1973 *J. Appl. Phys.* **44** 1281
[45] He X and Sun Z G 2017 *Mater. Rev.* **31** 6 (in Chinese)